Attribution of observed streamflow changes in key British Columbia drainage basins

Mohammad R. Najafi, Francis W. Zwiers, & Nathan P. Gillett

2017

Original citation:

Najafi, M. R., Zwiers, F. W., & Gillett, N. P. (2017). Attribution of observed streamflow changes in key British Columbia drainage basins. *Geophysical Research Letters*, *44*(21), 11012–11020. https://doi.org/10.1002/2017GL075016

AGU PUBLICATIONS

Geophysical Research Letters

RESEARCH LETTER

10.1002/2017GL075016

Key Points:
- Observed changes in BC's summer streamflow are inconsistent with simulations representing the responses to natural forcing factors alone
- The responses to ALL forcings as well as the anthropogenic forcing are detected
- BC's normalized summer streamflow changes are dominated by changes in the Fraser and Columbia River basins

Supporting Information:
- Supporting Information S1

Correspondence to:
M. R. Najafi,
mnajafi7@uwo.ca

Citation:
Najafi, M. R., Zwiers, F. W., & Gillett, N. P. (2017). Attribution of observed streamflow changes in key British Columbia drainage basins. *Geophysical Research Letters*, *44*, 11,012–11,020. https://doi.org/10.1002/2017GL075016

Received 14 OCT 2016
Accepted 12 OCT 2017
Accepted article online 16 OCT 2017
Published online 2 NOV 2017

Attribution of Observed Streamflow Changes in Key British Columbia Drainage Basins

Mohammad Reza Najafi[1,2], Francis W. Zwiers[1], and Nathan P. Gillett[3]

[1]Pacific Climate Impacts Consortium, University of Victoria, Victoria, BC, Canada, [2]Department of Civil and Environmental Engineering, The University of Western Ontario, London, ON, Canada, [3]Canadian Centre for Climate Modelling and Analysis, Environment and Climate Change Canada, Victoria, BC, Canada

Abstract We study the observed decline in summer streamflow in four key river basins in British Columbia (BC), Canada, using a formal detection and attribution (D&A) analysis procedure. Reconstructed and simulated streamflow is generated using the semidistributed variable infiltration capacity hydrologic model, which is driven by 1/16° gridded observations and downscaled climate model data from the Coupled Model Intercomparison Project phase 5 (CMIP5), respectively. The internal variability of the regional hydrologic components using ~5100 years of streamflow was simulated using CMIP5 preindustrial control runs. Results show that the observed changes in summer streamflow are inconsistent with simulations representing the responses to natural forcing factors alone, while the response to anthropogenic and natural forcing factors combined is detected in these changes. A two-signal D&A analysis indicates that the effects of anthropogenic (ANT) forcing factors are discernable from natural forcing in BC, albeit with large uncertainties.

1. Introduction

Nival and glacier-fed rivers in western Canada have low flows in winter when precipitation falls primarily as snow, high flows in spring when the snowpack melts, and gradually declining flows after midsummer as snowmelt diminishes. The accumulated spring snowpack plays a prominent role in the region's hydrologic regime by modulating the spring freshet and summer streamflow. Therefore, warming temperatures and the consequent changes in winter snow storage threaten water resources in the summer dry season (Clow, 2010; Stahl & Moore, 2006).

Historical streamflow records in different places around the globe show divergent trends (Alkama et al., 2013), with both increases and decreases being reported (Labat et al., 2004; Dai et al., 2009). This is partly because multiple factors determine how streamflow responds to the warming climate, including a basin's mean elevation, vegetation cover, and water balance changes. Warming has generally reduced the snowpack and increased snowmelt at low and middle elevations of the Northern Hemisphere (NH) midlatitudes, albeit at a lower rate at high elevations where the temperature stays below freezing (Mote, 2003; Stewart, 2009) (see also Vaughan et al., 2013, Figure 4.20).

In western North America, studies show earlier snowpack depletion (Mote et al., 2005; Mote, 2006; Kang et al., 2014; Najafi et al., 2016), increased April mean streamflow (Vincent et al., 2015), reduced summer streamflow, earlier streamflow center of timing, and an earlier spring freshet (Déry et al., 2009; Kang et al., 2016; Stewart et al., 2004; Zhang et al., 2001). More pronounced changes in streamflow timing are expected in the future with projected temperature increases (Maurer et al., 2007; Najafi & Moradkhani, 2014, 2015; Schnorbus et al., 2014).

Warming both globally and regionally has been attributed to anthropogenic influences, including at high northern latitudes, in the U.S. Pacific Northwest, and Canadian regions (Abatzoglou et al., 2014; Hegerl et al., 2007; Jones et al., 2013; Najafi et al., 2015). Impacts on the hydrologic cycle have been detected in the zonal mean distribution of precipitation (Marvel & Bonfils, 2013; Zhang et al., 2007) and at high northern latitudes (Min et al., 2008), NH snow cover extent (Najafi et al., 2016; Rupp, Mote, et al., 2013), and western United States and British Columbia (BC) snow mass (Barnett et al., 2008; Fyfe et al., 2017; Najafi et al., 2017). Nevertheless, very few studies have detected an anthropogenic signal in streamflow changes. Maurer et al. (2007) studied the center of timing (CT) of streamflow in four Sierra Nevada river basins and did not find evidence to conclude that observed CT trends were inconsistent with internal variability. Using two global climate models Hidalgo et al. (2009) similarly did not detect anthropogenic responses in

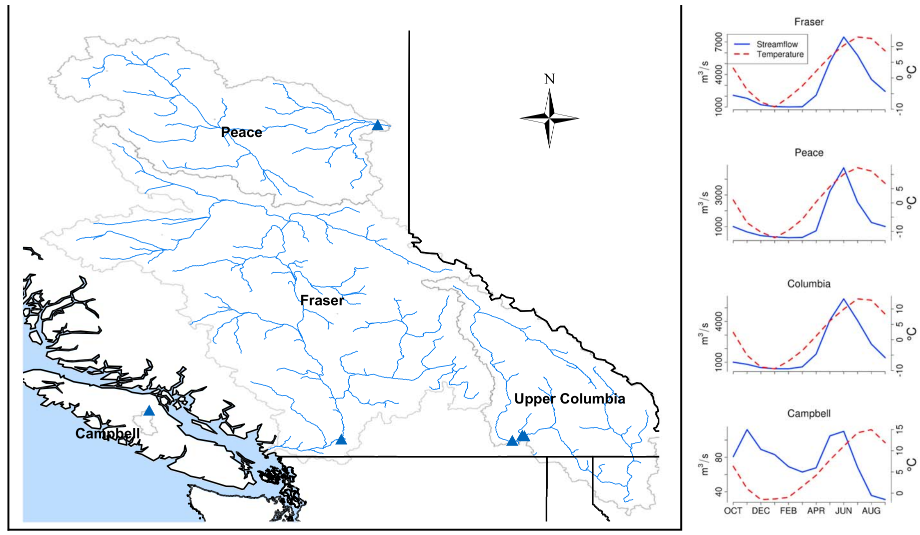

Figure 1. (left) Study area and (right) observed monthly mean temperature and streamflow climatology. Gridded observed temperature at 1/16° resolution is spatially averaged over each river basin for 1951–2005; naturalized streamflow records (except Slocan River near Crescent Valley with natural flow measurements) from gauging stations representative of each basin are available for 1958–2005 (Fraser at Hope), 1984–2005 (Columbia, representing the aggregated flow rate from three stations), 1968–1997 (Peace at Taylor), and 1963–2005 (Campbell at Strathcona Dam).

the CT of the Sacramento, San Joaquin, and Upper Colorado River basins. Evidence that anthropogenic influence had advanced the CT did emerge when they considered an expanded region that included the Columbia River basin. In another study over the western U.S., Barnett et al. (2008) found human influence in the joint variability of 1 April snow water equivalent (normalized by annual precipitation), January-February-March minimum temperature, and CT.

Previous studies were conducted in water-limited regions of western North America. We focus here on an energy-limited region with distinct terrestrial hydrological sensitivity (Kumar et al., 2016). Major BC river basins accumulate snow from October to March, providing natural water storage that supplies various stakeholders during summer. Changes in the regional hydrologic cycle associated with warming can cause water management issues. We study June-July-August (JJA) changes because stakeholder water demand is high and observed streamflow declines are proportionally large. We conduct hydrologic simulations of four BC drainage basins based on a suite of Coupled Model Intercomparison Project phase 5 (CMIP5) simulations to determine whether anthropogenic influence has contributed to observed summer streamflow changes. We also test the sensitivity of detection and attribution (D&A) results to the effects of Pacific Decadal Oscillation (PDO) since observed temperature (Vincent et al., 2015) and streamflow (Gurrapu et al., 2016) variations in western Canada have been linked with the Pacific Decadal Oscillation (PDO).

2. Data

Our study area includes the Fraser (drainage area ~230,000 km^2), Peace (101,000 km^2), upper Columbia (86,400 km^2), and Campbell River (1193 km^2) basins (Figure 1). We use observed daily minimum temperature, maximum temperature, and precipitation records gridded to 1/16° spatial resolution (Schnorbus et al., 2011). Daily streamflow records were acquired from high-quality gauging stations representative of each basin; these are located on the Fraser River at Hope, the Peace River at Taylor, and the Campbell River at Strathcona Dam, as well as the Columbia River at Keenlyside Dam, Kootenay River at Kootenay Canal, and Slocan River near Crescent Valley (SRCV). Records from the three Columbia River basin stations were aggregated into a single time series by summing the daily discharge rates as they showed similar flow timing. All flow records are affected by regulation (except SRCV), and thus, we used naturalized streamflow data provided by BC Hydro (Schnorbus et al., 2011). All basins have nival characteristics, except the Campbell, a low-elevation coastal basin with a hybrid nival/pluvial regime (Figure 1, right).

We use climate simulations from 10 CMIP5 (Taylor et al., 2012) models. This includes climate simulations forced by historical changes in anthropogenic (greenhouse gases, aerosols, ozone, and land cover) and natural (solar output and volcanic activity) forcing factors (ALL; 40 simulations), an equal number of simulations with natural (NAT) external forcing alone (40 simulations), and preindustrial control (CTL) simulations that are used to assess internal climate variability (>5100 years in total, divided into 93 55 year chunks). The CMIP5 models used in this study are BCC-CSM1-1 (1,1,7), CanESM2 (5,5,14), CCSM4 (4,4,16), CNRM-CM5 (6,6,11), CSIRO-Mk3-6-0 (5,5,7), GFDL-CM3 (3,3,7), GISS-E2-R-CC (10,10,17), HadGEM2-ES (4,4, −), MRI-CGCM3 (1,1,7), and NorESM1-M (1,1,7), where numbers in parentheses indicate the ALL, NAT, and CTL chunk ensemble size, respectively. The performance of these models varies at the regional scale (Rupp, Abatzoglou, et al., 2013). A statistical downscaling procedure (see section 3) helps to reduce some biases, including those in variability, but some biases may remain, such as in the distribution of variance across time scales, which is a source of uncertainty in the regional D&A analysis.

3. Methods

Daily precipitation (P), maximum temperature (T_{max}), minimum temperature (T_{min}), and wind speed (W) at 1/16° spatial resolution are required to drive the hydrologic model used in this study. Simulated monthly mean P, T_{max}, and T_{min} were obtained from the ALL, NAT, and CTL simulations and downscaled to the spatiotemporal resolution of the observed gridded data set using the bias correction and spatial disaggregation (BCSD) method considering 1943–2005 as the training period (Maurer & Hidalgo, 2008; Wood et al., 2002). Because insufficient in situ wind is available, we obtained the necessary 10 m wind speed data from the National Centers for Environmental Prediction–National Center for Atmospheric Research reanalysis (Kalnay et al., 1996), which was regridded to the same 1/16° resolution similar to Hamlet and Lettenmaier (2005), Maurer et al. (2002), and Wood et al. (2002). As in other studies, we used the reanalyzed wind forcing data set for all simulations, assuming that wind speed changes have a negligible impact on summer streamflow over the historical period we analyze. Consistent with previous studies, short-wave radiation and humidity were estimated from T_{min} and T_{max} using the Mountain Microclimate Simulation Model, and long-wave radiation was estimated from humidity and temperature using Tennessee Valley Authority algorithms (Liang et al., 1996). The downscaled data were used to drive the semidistributed variable infiltration capacity (VIC) hydrologic model (Liang et al., 1994, 1996) to generate daily runoff and base flow time series at each grid cell. Subsequently, a flow routing scheme based on the linearized St. Venant's equations (Lohmann et al., 1998, 1996) was used to simulate flow at the selected gauging stations (shown in Figure 1). This was repeated for each of 173 CMIP5 simulations (40 ALL, 40 NAT, and 93 CTL chunks) over the individual river basins, resulting in 692 hydrologic simulations for the period of 1943–2005, with the initial 7 years considered as the spin-up period. Simulated streamflow from the calibrated VIC model driven by BCSD downscaled data has previously been evaluated and utilized for the assessment of future climate change impacts on streamflow in the region (Schnorbus et al., 2011; Shrestha et al., 2012, 2014); these studies found that VIC-BCSD simulated streamflow agreed well with observed streamflow over a 1961–1990 baseline period.

To better isolate the impact of temperature-driven snow storage changes on streamflow, we based our D&A analysis on normalized summer streamflow (NQ). NQ is defined as the ratio of the cumulative summer (June-July-August (JJA)) discharge volume in each year (expressed as an equivalent daily precipitation rate) to the mean daily precipitation rate for the year commencing the preceding 1 September. NQ represents the fraction of the total basin precipitation input during the antecedent cold period and subsequent summer that is discharged during that summer. We assume that precipitation from prior water years does not contribute to JJA streamflow in the current water year.

We analyze historical NQ changes using reconstructed (denoted NQ_{rec}) rather than directly observed streamflow observations because the available naturalized streamflow records cover different time periods (e.g., 1984–2005 in the Columbia and 1968–1997 in the Peace River basin) and are not generally long enough to allow robust attribution. Streamflow is reconstructed for 1951–2005 by driving VIC with gridded observed P, T_{min}, T_{max}, and W. Assessment of the linear trends in simulated and reconstructed NQ was conducted using Sen's nonparametric slope estimator, and the statistical significance of the trend estimates was assessed based on the Mann-Kendall test after accounting for year-to-year persistence following Zhang et al. (2000).

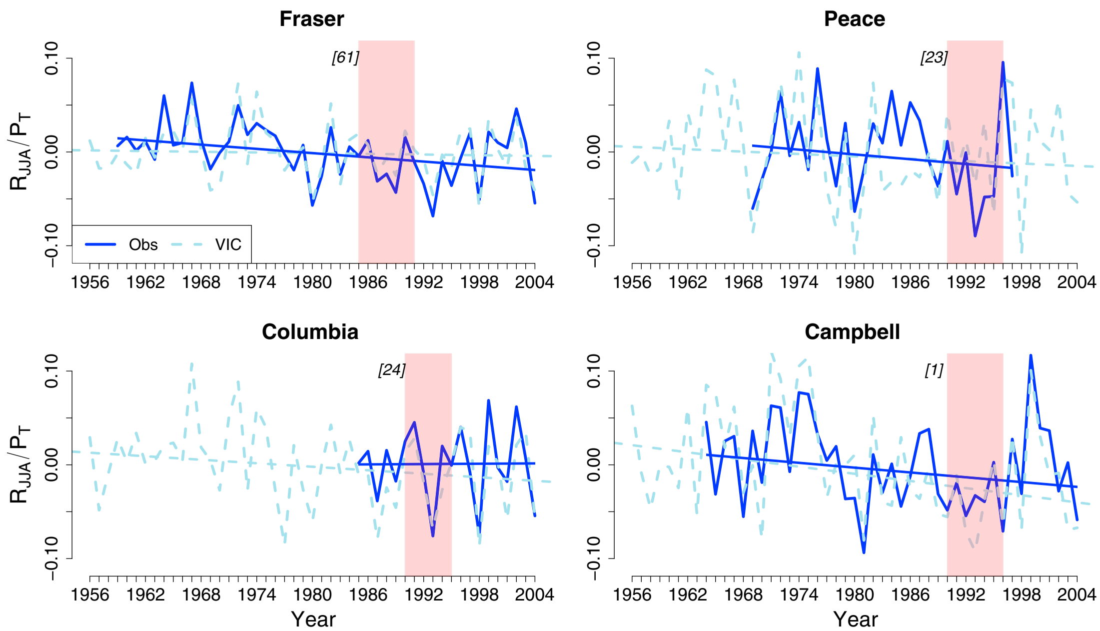

Figure 2. Variability and trend of observed (naturalized; natural for Slocan River near Crescent Valley) and VIC-reconstructed anomalies of cumulative summer (JJA) streamflow normalized by annual precipitation. Shaded bands show the calibration period. Numbers in the top left of the shaded bands indicate the number of gauging sites used for calibration in each basin.

We assessed whether changes in nonoverlapping 5 year NQ_{rec} means are significantly different from internal variability (i.e., detection) and whether those changes can be attributed to the anthropogenic forcing effects using an optimal fingerprinting approach (Allen & Stott, 2003; Ribes & Terray, 2013). Time averaging reduces the effects of internal unforced variability (noise) on long-term streamflow changes and increases the signal-to-noise ratio, which helps detect anthropogenic and natural forcing effects. It is also desirable to keep the dimensionality of the D&A problem small in order to better estimate the covariance matrix of internal variability.

The D&A method projects vectors composed of 5 year mean NQ_{rec} values onto corresponding 5 year mean multimodel ensemble averages of the simulated NQ responses to external climate forcing (i.e., NQ_{ALL} and NQ_{NAT}) with a generalized linear regression model using the total least squares approach:

$$NQ_{rec} = \beta_1 NQ_{ALL} + \beta_2 NQ_{NAT} + \Delta \tag{1}$$

where $NQ_{ALL} = NQ^*_{ALL} + \varepsilon_{NQ_{ALL}}$ and $NQ_{NAT} = NQ^*_{NAT} + \varepsilon_{NQ_{NAT}}$.

The residual vectors Δ and ε represent the internal variability components of NQ_{rec}, NQ_{ALL}, and NQ_{NAT}, respectively. NQ_{ALL} and NQ_{NAT} are obtained as multimodel ensemble means of finite numbers of climate simulations. NQ^*_{ALL} and NQ^*_{NAT} represent the means of corresponding infinite populations of ALL and NAT simulations. Scaling factors corresponding to the effect of anthropogenic (ANT) forcing and NAT signals, and their respective confidence intervals, are estimated by decomposing NQ_{ALL} into $NQ_{ALL} = NQ_{ANT} + NQ_{NAT}$, which results in $\beta_{ANT} = \beta_1$ and $\beta_{NAT} = \beta_1 + \beta_2$. A signal is detected in observations when the 5%–95% confidence interval for its scaling factor exceeds zero. Scaling factors close to unity with small uncertainty ranges imply that the observed changes may be partly attributable to the corresponding forcing factors.

4. Results

We used a version of the VIC hydrologic model that has been set up and calibrated at the Pacific Climate Impacts Consortium (Schnorbus et al., 2011; Shrestha et al., 2012). The model was calibrated against 5 years of daily streamflow data from multiple gauging sites within each basin (except the small Campbell Basin,

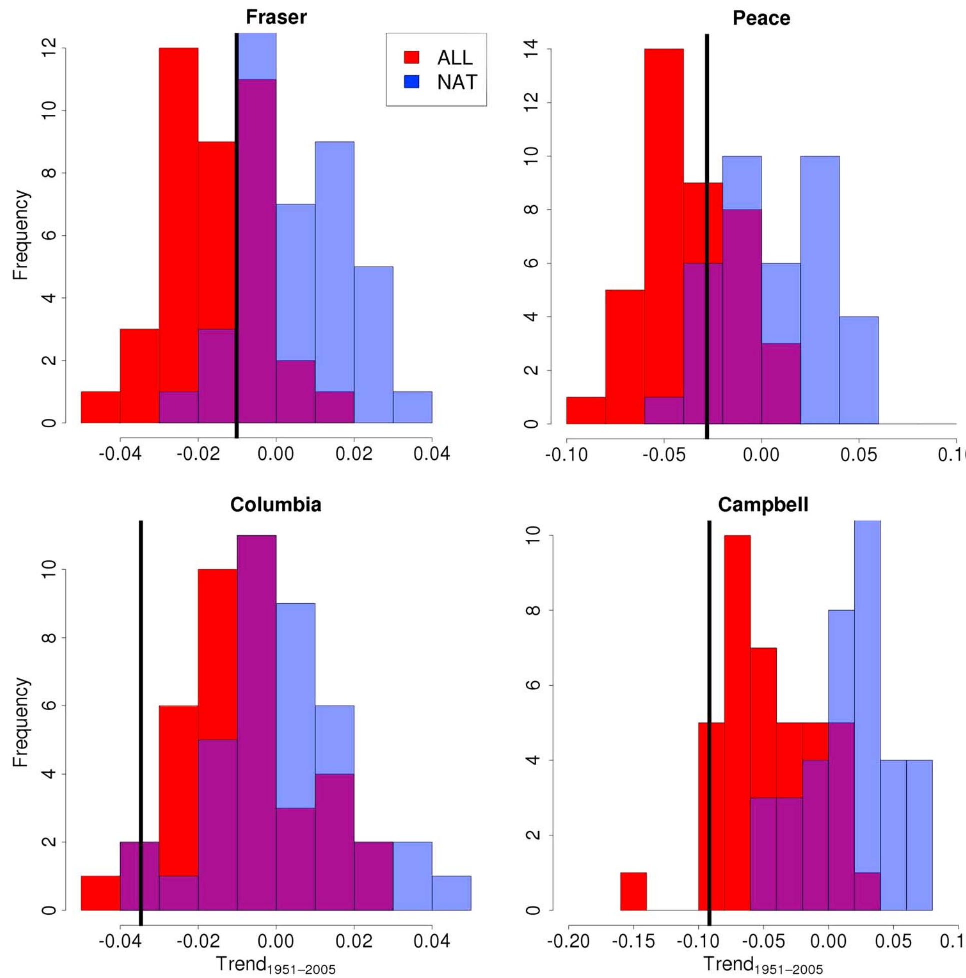

Figure 3. Linear trends of the normalized summer streamflow obtained from reconstructed observations (vertical black bar), a 40-member ensemble of hydrologic simulations driven by downscaled climate simulations that include natural (NAT) external forcing factors (blue bars) and a 40-member ensemble of hydrologic simulations driven by downscaled climate simulations that include anthropogenic and natural forcing factors combined (ALL; red bars) for 1951–2005; overlapping bars are colored "purple."

where only one gauging site is available) using multiple objective metrics. The selected calibration period is a trade-off between the length of the period and other constraints such as a desire to use Water Survey of Canada records in as many subwatersheds as possible and the same calibration period at all locations to ensure homogeneity. Values of Kling-Gupta (Gupta et al., 2009) and Nash-Sutcliffe efficiencies (in parentheses) for the reconstructed monthly streamflows are 0.89 (0.93), 0.89 (0.88), 0.86 (0.83), and 0.83 (0.68) for the Fraser, Peace, Columbia, and Campbell River basins, respectively. Corresponding values for summer streamflow reconstructions are 0.86 (0.82), 0.71 (0.67), 0.78 (0.44), and 0.76 (0.67), indicating acceptable model performance (see also Figure S1 in the supporting information). Low flows tend to be underestimated for the Fraser and Columbia, with a similar tendency for high flows in the Peace Basin. Analysis of individual months (shown in Table S1 in the supporting information) shows that the model performs best during October and worst during February. The number of gauging sites used for calibration is indicated in Figure 2. The model reproduces NQ interannual variability well in all basins (Figure 2), with observed to reconstructed NQ variance ratios that are consistent with unity based on the *F*-statistic. Inconsistencies in model simulations (i.e., NQ overestimation in 1980s and underestimation in early 1990s in the Peace) may be due to gridded precipitation data that are based on limited station observations.

Observed NQ exhibits declining trends in three of four basins (the Columbia trend is close to zero (+0.0006/decade)), with the largest observed decline (−0.009/decade) occurring in the Campbell Basin. Note however

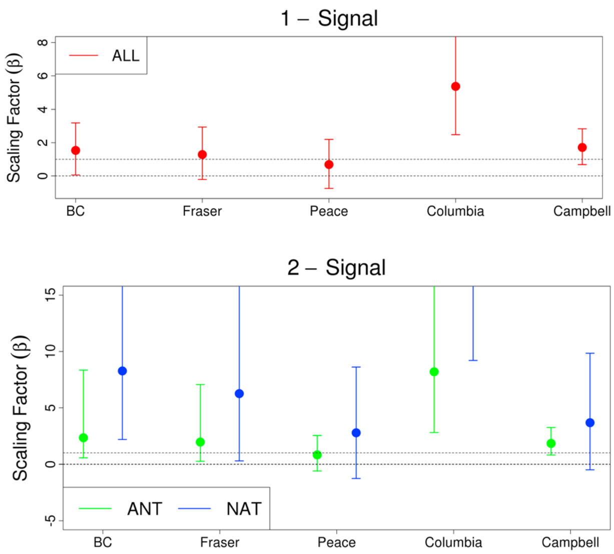

Figure 4. Scaling factors and their corresponding 5%–95% confidence intervals (top) for anthropogenic and natural forcing factors combined (ALL) in a one-signal D&A analysis and (bottom) for anthropogenic (ANT) forcings and natural (NAT) forcings in a two-signal analysis, based on the normalized summer streamflow 1951–2005.

that trends based on short two-decade periods are more uncertain than those based on longer periods. Trends in reconstructed NQ (NQ_{rec}) over the periods when observed NQ is available differ marginally from those in observed NQ (Figure 2). Trends in NQ_{rec} over the 1951–2005 period are negative in all basins, with the largest trend seen in the Campbell Basin. The trend differences between observed and reconstructed NQ arise from uncertainties in hydrologic model formulations (i.e., structural), calibration (i.e., parametric), and observations. The latter is likely dominated by the sparsity and uneven vertical distribution of the station data that underlie the driving gridded climate observations.

We compare trends in NQ_{rec} with those simulated by VIC when driven by downscaled climate simulations that account only for natural (NAT) external forcing and when driven by climate simulations that account for anthropogenic and natural external forcings combined (ALL) (Figure 3). A majority of streamflow simulations that include anthropogenic forcing show negative trends, with almost all such simulations showing negative trends in the Fraser, Peace, and Campbell, and with good agreement between simulated trends and those in the reconstructed observations. In contrast, the NAT simulations exhibit trends that are generally inconsistent with NQ_{rec} in all basins, with trend distributions that are roughly centered on zero. The observed trends lie close to the lower tails of the NAT simulations in the Fraser and Peace River basins and outside the range of these trends in the Campbell River basin. The ALL simulations tend to show smaller declining trends in the Columbia River basin compared to NQ_{rec}. While the NQ_{rec} trends lie close to the lower tails of both ALL and NAT simulations, they show more consistency with ALL. This basin is located at a relatively high altitude (mean elevation of 1600 m), where there are larger inconsistencies between the observed and simulated snowpack (Najafi et al., 2017).

To conduct the D&A analysis, we use 5 year NQ_{rec}, NQ_{ALL}, NQ_{NAT}, and NQ_{CTL} averages (Figure S2). There is a generally consistent pattern of change in NQ_{rec} between the four river basins due to their spatial proximity (for example, they all show peaks in 1971–1975 and 1996–2000; the PDO evidently affects the regional temperature in all basins; Figure S3). Nevertheless, the overall response to the long-term warming trend and the subsequent snowpack changes vary due to topographic differences between basins. The multimodel mean response to ALL forcing shows a decreasing trend in all basins, particularly during the period of more rapid warming after 1975. In contrast, the multimodel mean response to NAT forcing shows little change. For an overall assessment of anthropogenic influence on NQ_{rec}, we aggregate NQ from all four river basins, weighted by drainage area for NQ_{rec}, NQ_{ALL}, NQ_{NAT}, and NQ_{CTL}.

Our null hypothesis is that the pattern of change in NQ_{rec} is due to internal variability. A one-signal D&A analysis detects the response to ALL forcing in aggregated NQ_{rec}, as shown by the scaling factor and its 90% confidence interval, which lies above zero (Figure 4). The ALL forcing simulated changes are consistent with observed changes since the scaling factor is not statistically distinguishable from unity. The response to ALL forcing is also detected in the Campbell and Columbia River basins, although the scaling factor for the Columbia has high uncertainty and is significantly greater than unity. The latter indicates that NQ_{rec} changes are underestimated by the ALL forcing simulations for the Columbia River. While scaling factors are consistent with unity in the Fraser and Peace Basins, the response to ALL forcing is not detected due to large uncertainties in the scaling factor estimates, which is likely due to large, unforced internal variability. Consequently, the impact of climate change is detected via one-signal D&A analysis in the aggregated, Campbell River and Columbia River basin NQ_{rec}.

We next conducted a two-signal D&A analysis that simultaneously projects NQ_{rec} onto the multimodel mean-simulated responses to ALL and NAT forcings. Both ANT and NAT signals are detected in the four-basin aggregated data, albeit with large uncertainty, which likely stems from the inclusion of the small, and thus relatively more uncertain, NAT signal in the analysis (Ribes et al., 2015). ANT is also detected in the Fraser and Campbell River basins, but it is not detected in the Peace Basin. Disaggregating the Fraser ALL signal into ANT and NAT components allows ANT to be detected even though the combined ALL signal cannot be detected. In the Columbia River basin ANT is detected, but as with the one-signal analysis, its scaling factor is inconsistent with unity, indicating that the CMIP5-driven VIC simulations underestimate the ANT signal for this basin. The scaling factors corresponding to NAT are consistent with zero in the Peace and Campbell Basins indicating no detectable response to natural external forcing in these basins.

Our findings of anthropogenic influence on NQ_{rec} are robust to the choice of regression technique. The results described above were obtained with the total least squares (TLS) regression model (Allen & Stott, 2003; Ribes & Terray, 2013). We also conducted one- and two-signal D&A analyses for the aggregated data using the ordinary least squares regression method (e.g., Allen & Tett, 1999) (Figure S4). An anthropogenic signal is again identified in NQ_{rec}, while the NAT signal scaling factor is found to be consistent with zero, indicating that detection of NAT based on the TLS approach may not be robust. Our findings are also robust to the effects of the low-frequency variability related to the PDO (Figure S5).

5. Conclusions

We analyzed observed and reconstructed normalized summer streamflow in four BC river basins representing a drainage area of about 430,000 km^2 and compared it with simulated summer streamflow under recent historical anthropogenic and natural external forcings. Our results suggest that observed summer streamflow declines in these basins are attributable to anthropogenic climate change. Linear trends in normalized summer streamflow simulated when accounting for both natural and anthropogenic forcings are consistent with those in the reconstructed observations and show declines in all four river basins for 1951–2005, while trends in simulations that include only natural forcings are close to zero. Using a formal detection and attribution approach, we find that reconstructed summer streamflow changes are consistent with the simulated effects of anthropogenic and natural forcings combined. We also detect the response to the anthropogenic forcing at the 5% significance level. BC's normalized summer streamflow declines are dominated by changes in the Fraser and Columbia River basins A strong anthropogenic influence is also detected in the Campbell River basin, but its overall contribution to aggregated streamflow changes is limited because of its small drainage area. We did not detect an anthropogenic influence on Peace River streamflow.

We account for climate uncertainty by using a large set of climate simulations from 10 global climate models. There are other sources of uncertainties in the climate impact modeling chain including downscaling and bias correction, hydrological model structure, and parameterization (Mendoza, Clark, Mizukami, Gutmann, et al., 2015; Mendoza, Clark, Mizukami, Newman, et al., 2015; Mendoza et al., 2016; Mizukami et al., 2016; Najafi et al., 2011). Although climate models are likely the largest contributors to overall uncertainty (Ahn et al., 2016; Najafi et al., 2011), there are other important sources of uncertainty. The downscaling approach reduces some biases from the driving climate model, using different bias adjustments for each model, and the hydrologic calibration approach reduces biases from the hydrologic model (Figure S1). It must be recognized, however, that observational uncertainty in these constraints is largely irreducible. Future research should use a variety of downscaling and hydrological modeling frameworks to assess the magnitude of these sources of uncertainty. This includes consideration of dynamical downscaling approaches that explicitly represent mesoscale processes and feedback, and snow albedo feedback processes that affect the snowpack in high-elevation regions (Rupp et al., 2017).

Detection of an anthropogenic influence on normalized summer streamflow in BC is consistent with previous findings that human influence has caused a decline in the 1 April snowpack. Water stored in the form of snow during the cold season plays a significant role in spring and summer streamflow in nival (Columbia, Fraser, and Peace) and hybrid (Campbell) river basins, with reduced snowpack corresponding to lower summer streamflow. These analyses, combined with previous findings for the western U.S. (Barnett et al., 2008; Hidalgo et al., 2009), suggest that human influence has altered the hydrology of both energy-limited (western Canada) and water-limited (western U.S.) regions (Kumar et al., 2016) of western North America.

Acknowledgments
We thank Alex Cannon, Markus Schnorbus, Arelia Werner, Rajesh Shrestha, and Sanjiv Kumar for their help with the modeling setup. We also thank Xuebin Zhang and Alex Cannon for their helpful comments. Funding for this project is provided by the Canadian Sea Ice and Snow Evolution (CanSISE) project. CMIP5 data are publically available via http://cmip-pcmdi.llnl.gov/cmip5/data_portal.html. We used VIC version 4.1.2g as implemented and calibrated at PCIC. Observed and simulated data used in this study can be downloaded from https://pacificclimate.org/~fwzwiers/Najafi-et-al-stream-flow/.

References

Abatzoglou, J. T., Rupp, D. E., & Mote, P. W. (2014). Seasonal climate variability and change in the Pacific Northwest of the United States. *Journal of Climate*, *27*(5), 2125–2142.

Ahn, K. H., Merwade, V., Ojha, C. S. P., & Palmer, R. N. (2016). Quantifying relative uncertainties in the detection and attribution of human-induced climate change on winter streamflow. *Journal of Hydrology*, *542*, 304–316.

Alkama, R., Marchand, L., Ribes, A., & Decharme, B. (2013). Detection of global runoff changes: Results from observations and CMIP5 experiments. *Hydrology and Earth System Sciences Discussions*, *10*(2), 2117–2140.

Allen, M., & Stott, P. (2003). Estimating signal amplitudes in optimal fingerprinting, part I: Theory. *Climate Dynamics*, *21*(5-6), 477–491.

Allen, M. R., & Tett, S. F. (1999). Checking for model consistency in optimal fingerprinting. *Climate Dynamics*, *15*(6), 419–34.

Barnett, T. P., Pierce, D. W., Hidalgo, H. G., Bonfils, C., Santer, B. D., Das, T., … Mirin, A. A. (2008). Human-induced changes in the hydrology of the western United States. *Science*, *319*(5866), 1080–1083.

Clow, D. W. (2010). Changes in the timing of snowmelt and streamflow in Colorado: A response to recent warming. *Journal of Climate*, *23*(9), 2293–2306.

Dai, A., Qian, T., Trenberth, K. E., & Milliman, J. D. (2009). Changes in continental freshwater discharge from 1948 to 2004. *Journal of Climate*, *22*(10), 2773–2792.

Déry, S. J., Stahl, K., Moore, R., Whitfield, P., Menounos, B., & Burford, J. E. (2009). Detection of runoff timing changes in pluvial, nival, and glacial rivers of western Canada. *Water Resources Research*, *45*, W04426. https://doi.org/10.1029/2008WR006975

Fyfe, J. C., Derksen, C., Mudryk, L., Flato, G. M., Santer, B. D., Swart, N. C., … Scinocca, J. (2017). Large near-term projected snowpack loss over the western United States. *Nature Communications*, *8*. https://doi.org/10.1038/ncomms14996

Gupta, H. V., Kling, H., Yilmaz, K. K., & Martinez, G. F. (2009). Decomposition of the mean squared error and NSE performance criteria: Implications for improving hydrological modelling. *Journal of Hydrology*, *377*(1-2), 80–91.

Gurrapu, S., St-Jacques, J. M., Sauchyn, D. J., & Hodder, K. R. (2016). The influence of the Pacific Decadal Oscillation on annual floods in the rivers of western Canada. *Journal of the American Water Resources Association*, *52*(5), 1031–1045.

Hamlet, A. F., & Lettenmaier, D. P. (2005). Production of temporally consistent gridded precipitation and temperature fields for the continental United States. *Journal of Hydrometeorology*, *6*(3), 330–336.

Hegerl, G., Zwiers, F., Braconnot, P., Gillet, N., Luo, Y., Marengo, J., … Stott, P. (2007). Understanding and attributing climate change. In S. Solomon, et al. (Eds.), *Climate change 2007: The physical science basis. Contribution of working group I to the fourth assessment report of the intergovernmental panel on climate change* (pp. 663–745). Cambridge, United Kingdom and New York: Cambridge University Press.

Hidalgo, H., Das, T., Dettinger, M., Cayan, D., Pierce, D., Barnett, T., … Bonfils, C. (2009). Detection and attribution of streamflow timing changes to climate change in the western United States. *Journal of Climate*, *22*(13), 3838–3855.

Jones, G. S., Stott, P. A., & Christidis, N. (2013). Attribution of observed historical near–surface temperature variations to anthropogenic and natural causes using CMIP5 simulations. *Journal of Geophysical Research: Atmospheres*, *118*, 4001–4024. https://doi.org/10.1002/jgrd.50239

Kalnay, E., Kanamitsu, M., Kistler, R., Collins, W., Deaven, D., Gandin, L., … Zhu, Y. (1996). The NCEP/NCAR 40-year reanalysis project. *Bulletin of the American meteorological Society*, *77*(3), 437–71.

Kang, D. H., Gao, H., Shi, X., ul Islam, S., & Déry, S. J. (2016). Impacts of a rapidly declining mountain snowpack on streamflow timing in Canada's Fraser River basin. *Scientific Reports*, *6*, 19299.

Kang, D. H., Shi, X., Gao, H., & Déry, S. J. (2014). On the changing contribution of snow to the hydrology of the Fraser River basin, Canada. *Journal of Hydrometeorology*, *15*(4), 1344–1365.

Kumar, S., Zwiers, F., Dirmeyer, P. A., Lawrence, D. M., Shrestha, R., & Werner, A. T. (2016). Terrestrial contribution to the heterogeneity in hydrological changes under global warming. *Water Resources Research*, *52*, 3127–3142.

Labat, D., Goddéris, Y., Probst, J. L., & Guyot, J. L. (2004). Evidence for global runoff increase related to climate warming. *Advances in Water Resources*, *27*(6), 631–642.

Liang, X., Lettenmaier, D. P., Wood, E. F., & Burges, S. J. (1994). A simple hydrologically based model of land surface water and energy fluxes for general circulation models. *Journal of Geophysical Research*, *99*, 14,415–14,415.

Liang, X., Wood, E. F., & Lettenmaier, D. P. (1996). Surface soil moisture parameterization of the VIC-2L model: Evaluation and modification. *Global and Planetary Change*, *13*(1–4), 195–206.

Lohmann, D., Nolte-Holube, R., & Raschke, E. (1996). A large-scale horizontal routing model to be coupled to land surface parameterization schemes. *Tellus A*, *48*(5), 708–721.

Lohmann, D., Raschke, E., Nijssen, B., & Lettenmaier, D. (1998). Regional scale hydrology: I. Formulation of the VIC-2L model coupled to a routing model. *Hydrological Sciences Journal*, *43*(1), 131–141.

Marvel, K., & Bonfils, C. (2013). Identifying external influences on global precipitation. *Proceedings of the National Academy of Sciences of the United States of America*, *110*(48), 19,301–19,306.

Maurer, E., Stewart, I., Bonfils, C., Duffy, P., & Cayan, D. (2007). Detection, attribution, and sensitivity of trends toward earlier streamflow in the Sierra Nevada. *Journal of Geophysical Research*, *112*, D11118. https://doi.org/10.1029/2006JD008088

Maurer, E., Wood, A., Adam, J., Lettenmaier, D., & Nijssen, B. (2002). A long-term hydrologically based dataset of land surface fluxes and states for the conterminous United States. *Journal of Climate*, *15*(22), 3237–3251.

Maurer, E. P., & Hidalgo, H. G. (2008). Utility of daily vs. monthly large-scale climate data: An intercomparison of two statistical downscaling methods. *Hydrology and Earth System Sciences*, *12*(2), 551–563.

Mendoza, P. A., Clark, M. P., Mizukami, N., Gutmann, E. D., Arnold, J. R., Brekke, L. D., & Rajagopalan, B. (2015). How do hydrologic modeling decisions affect the portrayal of climate change impacts? *Hydrological Processes*, *30*, 1071–1095. https://doi.org/10.1002/hyp.10684

Mendoza, P. A., Clark, M. P., Mizukami, N., Newman, A. J., Barlage, M., Gutmann, E. D., … Arnold, J. R. (2015). Effects of hydrologic model choice and calibration on the portrayal of climate change impacts. *Journal of Hydrometeorology*, *16*(2), 762–780.

Mendoza, P. A., Mizukami, N., Ikeda, K., Clark, M. P., Gutmann, E. D., Arnold, J. R., … Rajagopalan, B. (2016). Effects of different regional climate model resolution and forcing scales on projected hydrologic changes. *Journal of Hydrology*, *541*, 1003–1019.

Min, S.-K., Zhang, X., & Zwiers, F. (2008). Human-induced Arctic moistening. *Science*, *320*(5875), 518–520.

Mizukami, N., Clark, M. P., Gutmann, E. D., Mendoza, P. A., Newman, A. J., Nijssen, B., … Brekke, L. D. (2016). Implications of the methodological choices for hydrologic portrayals of climate change over the contiguous United States: Statistically downscaled forcing data and hydrologic models. *Journal of Hydrometeorology*, *17*(1), 73–98.

Mote, P. W. (2003). Trends in snow water equivalent in the Pacific Northwest and their climatic causes. *Geophysical Research Letters*, *30*(12), 1601. https://doi.org/10.1029/2003GL017258

Mote, P. W. (2006). Climate-driven variability and trends in mountain snowpack in western North America. *Journal of Climate*, *19*(23), 6209–6220.

Mote, P. W., Hamlet, A. F., Clark, M. P., & Lettenmaier, D. P. (2005). Declining mountain snowpack in western North America. *Bulletin of the American Meteorological Society*, *86*(1), 39–49.

Najafi, M. R., & Moradkhani, H. (2014). A hierarchical Bayesian approach for the analysis of climate change impact on runoff extremes. *Hydrological Processes*, *28*(26), 6292–6308. https://doi.org/10.1002/hyp.10113

Najafi, M. R., & Moradkhani, H. (2015). Multi-model ensemble analysis of runoff extremes for climate change impact assessments. *Journal of Hydrology*, *525*, 352–361.

Najafi, M. R., Moradkhani, H., & Jung, I. W. (2011). Assessing the uncertainties of hydrologic model selection in climate change impact studies. *Hydrological Processes*, *25*(18), 2814–2826.

Najafi, M. R., Zwiers, F., & Gillet, N. (2016). Attribution of the spring snow cover extent decline in Northern Hemisphere, Eurasia and North America to anthropogenic influence. *Climatic Change*, *136*(3-4), 571–586.

Najafi, M. R., Zwiers, F., & Gillett, N. (2017). Attribution of the observed spring snowpack decline in British Columbia to anthropogenic climate change. *Journal of Climate*, *30*(11), 4113–4130.

Najafi, M. R., Zwiers, F. W., & Gillett, N. (2015). Attribution of Arctic temperature change to greenhouse gas and aerosol influences. *Nature Climate Change*, *5*, 246–249.

Ribes, A., Gillett, N. P., & Zwiers, F. W. (2015). Designing detection and attribution simulations for CMIP6 to optimize the estimation of greenhouse gas–induced warming. *Journal of Climate*, *28*(8), 3435–8.

Ribes, A., & Terray, L. (2013). Application of regularised optimal fingerprinting to attribution. Part II: Application to global near-surface temperature. *Climate Dynamics*, *41*(11-12), 2837–2853.

Rupp, D. E., Abatzoglou, J. T., Hegewisch, K. C., & Mote, P. W. (2013). Evaluation of CMIP5 20th century climate simulations for the Pacific northwest USA. *Journal of Geophysical Research: Atmospheres*, *118*, 10,884–10,906. https://doi.org/10.1002/jgrd.50843

Rupp, D. E., Li, S., Mote, P. W., Shell, K. M., Massey, N., Sparrow, S. N., … Allen, M. R. (2017). Seasonal spatial patterns of projected anthropogenic warming in complex terrain: A modeling study of the western US. *Climate Dynamics*, *48*(7-8), 2191–2213.

Rupp, D. E., Mote, P. W., Bindoff, N. L., Stott, P. A., & Robinson, D. A. (2013). Detection and attribution of observed changes in Northern Hemisphere spring snow cover. *Journal of Climate*, *26*(18), 6904–6914.

Schnorbus, M., Bennett, K., Werner, A., & Berland, A. (2011). Hydrologic impacts of climate change in the Peace, Campbell and Columbia watersheds, British Columbia, Canada, *Pac. Clim*. Impacts Consort. Univ. Vic. Vic. BC, 157.

Schnorbus, M., Werner, A., & Bennett, K. (2014). Impacts of climate change in three hydrologic regimes in British Columbia, Canada. *Hydrological Processes*, *28*(3), 1170–1189.

Shrestha, R. R., Schnorbus, M. A., Werner, A. T., & Berland, A. J. (2012). Modelling spatial and temporal variability of hydrologic impacts of climate change in the Fraser River basin, British Columbia, Canada. *Hydrological Processes*, *26*(12), 1840–1860.

Shrestha, R. R., Schnorbus, M. A., Werner, A. T., & Zwiers, F. W. (2014). Evaluating hydroclimatic change signals from statistically and dynamically downscaled GCMs and hydrologic models. *Journal of Hydrometeorology*, *15*(2), 844–860.

Stahl, K., & Moore, R. (2006). Influence of watershed glacier coverage on summer streamflow in British Columbia, Canada. *Water Resources Research*, *42*, W06201. https://doi.org/10.1029/2006WR005022

Stewart, I. T. (2009). Changes in snowpack and snowmelt runoff for key mountain regions. *Hydrological Processes*, *23*(1), 78–94.

Stewart, I. T., Cayan, D. R., & Dettinger, M. D. (2004). Changes in snowmelt runoff timing in western North America under a business as usual' climate change scenario. *Climatic Change*, *62*(1–3), 217–232.

Taylor, K. E., Stouffer, R. J., & Meehl, G. A. (2012). An overview of CMIP5 and the experiment design. *Bulletin of the American Meteorological Society*, *93*(4), 485–498.

Vaughan, D. G., Comiso, J. C., Allison, I., Carrasco, J., Kaser, G., Kwok, R., … Zhan, T. (2013). Observations: Cryosphere. In T. F. Stocker, et al. (Eds.), *Climate change 2013: The physical science basis. Contribution of working group I to the fifth assessment report of the intergovernmental panel on climate change* (pp. 317–382). Cambridge, United Kingdom and New York: Cambridge University Press.

Vincent, L., Zhang, X., Brown, R., Feng, Y., Mekis, E., Milewska, E., … Wang, X. (2015). Observed trends in Canada's climate and influence of low-frequency variability modes. *Journal of Climate*, *28*(11), 4545–4560.

Wood, A. W., Maurer, E. P., Kumar, A., & Lettenmaier, D. P. (2002). Long-range experimental hydrologic forecasting for the eastern United States. *Journal of Geophysical Research*, *107*(D20), 4429. https://doi.org/10.1029/2001JD000659

Zhang, X., Harvey, K. D., Hogg, W., & Yuzyk, T. R. (2001). Trends in Canadian streamflow. *Water Resources Research*, *37*, 987–998. https://doi.org/10.1029/2000WR900357

Zhang, X., Vincent, L. A., Hogg, W., & Niitsoo, A. (2000). Temperature and precipitation trends in Canada during the 20th century. *Atmosphere-Ocean*, *38*(3), 395–429.

Zhang, X., Zwiers, F. W., Hegerl, G. C., Lambert, F. H., Gillett, N. P., Solomon, S., … Nozawa, T. (2007). Detection of human influence on twentieth-century precipitation trends. *Nature*, *448*(7152), 461–465.